



ELSEVIER

Available online at [www.sciencedirect.com](http://www.sciencedirect.com)

SCIENCE @ DIRECT®

Journal of Magnetism and Magnetic Materials 299 (2006) 75–81

Journal of  
magnetism  
and  
magnetic  
materials

[www.elsevier.com/locate/jmmm](http://www.elsevier.com/locate/jmmm)

# Spin-wave spectrum of copper metaborate in the incommensurate phase $T < 10$ K

S. Martynov<sup>a,\*</sup>, G. Petrakovskii<sup>a</sup>, M. Boehm<sup>b,c</sup>, B. Roessli<sup>b</sup>, J. Kulda<sup>c</sup>

<sup>a</sup>*Institute of Physics, SB RAS, 660036 Krasnoyarsk, Russian Federation*

<sup>b</sup>*Laboratory for Neutron Scattering, ETH Zurich & Paul Scherrer Institute, CH-5232 Villigen PSI, Switzerland*

<sup>c</sup>*Institute Laue-Langevin, 38042 Grenoble, Cedex 9, France*

Received 23 December 2004; received in revised form 18 March 2005

Available online 19 April 2005

## Abstract

The high-energy branch of the spin-wave spectrum of  $\text{CuB}_2\text{O}_4$  in the incommensurate magnetic phase was investigated by means of a linear spin-wave theory. The influence of the intersubsystem interactions on the spectrum of the “strong” subsystem was taken into account as the effective field in the framework of the mean-field approach. The comparison with the inelastic neutron scattering experiment leads to the conclusion about the additional “spiral anisotropy” appearance due to the dynamical interaction through the “weak” subsystem fluctuations (the “order due to disorder” mechanism) in the incommensurate phase.

© 2005 Elsevier B.V. All rights reserved.

PACS: 75.25.+z; 75.10.Hk; 75.30.Gw

Keywords: Spin-wave spectrum; Inelastic neutron scattering; Copper metaborate; Incommensurate structure

## 1. Introduction

Intensive investigations of the magnetic structure of copper metaborate  $\text{CuB}_2\text{O}_4$  during the last few years have revealed the existence of different types of magnetic ordering with a series of phase transitions as a function of both temperature and magnetic field [1–7]. The variety of magnetic

structures can be explained by the existence in this substance of two  $\text{Cu}^{2+}$  ions spin subsystems, which are completely different. This difference first of all is related to the strength of the main magnetic interactions within each subsystem. Antiferromagnetic (AF) exchange interaction between  $\text{Cu}^{2+}$  ions located at 4b crystallographic positions with point symmetry  $S_4$  forms the three-dimensional magnetic subsystem A with the Neel temperature  $T_{\text{N1}} = 20$  K. The average moment value of  $\text{Cu}^{2+}$  ions in A-sites increases rapidly below  $T_{\text{N1}}$  and reaches  $0.94 \mu_{\text{B}}$  at  $T = 2$  K. The magnetic moment

\*Corresponding author. Tel.: +7 391 2432635;  
fax: +7 391 2438923.

E-mail address: [UnonaV@iph.krasn.ru](mailto:UnonaV@iph.krasn.ru) (S. Martynov).

of copper magnetic ions in the B-subsystem are located at 8d positions (point symmetry  $C_2$ ) and reaches only  $0.54 \mu_B$  at the same temperature. Such a reduction of the value of the moment when  $T \rightarrow 0$  K in comparison with the saturation value of the free  $S = \frac{1}{2}Cu^{2+}$  ion is the signature of either quasi low-dimensional [8] or frustrated [9] exchange interactions in this subsystem. The analysis of the exchange interactions in B-subsystem showed the existence of dominant AF interactions which formed zig-zag ladder chains along the tetragonal axis [11]. The analysis of the spin-wave (SW) spectrum of both subsystems at  $T = 12$  K in the previous papers [10,11] led to the conclusion that interactions between subsystems has a weak influence on the dynamical properties of copper metaborate in this temperature range. The consideration of the possible super-exchange pathways Cu–O–B–O–Cu in  $CuB_2O_4$  shows that AF interactions between A- and B-subsystem are completely frustrated for AF orientation of the moments within each subsystem. It is the reason for the quasi-decoupled behavior of the two subsystems. Below  $T_s \approx 10$  K the magnetic structure of  $CuB_2O_4$  is incommensurate along the tetragonal axis with propagation vector which rises continuously from  $k = 0$  to  $k = 0.15$  rlu (reduced lattice units) with decreasing temperature [3,4]. This change in the magnetic structure leads to the breaking of frustration between the intersubsystem exchange interactions and, as a result, to the increase of the influence of these interactions on the dynamical properties. The frustration-breaking leads to the appearance of the gap in the SW spectrum of the A-subsystem, observed with inelastic neutron scattering experiments. The inelastic neutron scattering experiments were performed at the Institut Laue Langevin (ILL), Grenoble, at the thermal triple-axis spectrometer IN22. The experimental details were described in our first paper [10].

## 2. Exchange interactions

In order to take into account the influence of the intersubsystem interactions on the SW spectrum,

we consider the equilibrium orientations of the  $Cu^{2+}$  spins in both subsystems within the mean field approach. The Hamiltonian of the model

$$\begin{aligned}
 H = & J_a \sum_a \vec{S}_i \vec{S}_{i'} + J_{b1} \sum_b \vec{S}_j \vec{S}_{j+1} \\
 & + J_{b2} \sum_b \vec{S}_j \vec{S}_{j+2} \\
 & + J_{ab} \sum_{ab} \vec{S}_i \vec{S}_j + D_{b1} \sum_b [\vec{S}_j \times \vec{S}_{j+1}]_z \\
 & + D_{ab} \sum_{ab} [\vec{S}_i \times \vec{S}_j]_z
 \end{aligned} \quad (1)$$

includes AF exchange interactions between nearest-neighbors (NN) in both subsystems, AF interaction between next-nearest-neighbors (NNN) in B-subsystem, an AF exchange interaction between the two subsystems ( $J_{ab}$ ) and antisymmetrical exchange interactions between NN both in the B-subsystem ( $D_b$ ) and between subsystems ( $D_{ab}$ ). The allowance for the last two interactions follows from the analysis of the Lifshitz invariant of the thermodynamical potential for copper metaborate symmetry [4,12]. The Dzyaloshinskii–Moriya interaction between A-ions, antisymmetrical exchange interactions between NNN in B-subsystem and exchange interaction between ladders are neglected for simplicity. In Eq. (1) the exchange interaction between A- and B-ions ( $J_{ab}$ ) is considered between ions which are separated by the distance  $\Delta z = c/8$  only (NN along the tetragonal axis). The A-subsystem is considered as an easy-plane anti-ferromagnet ( $J_a^x = J_a^y = J_a^{xy} > J_a^z$ ) [11] with the equilibrium orientation of the magnetic moments within the tetragonal plane of the crystal. Fig. 1 shows a simple representation of the exchange interactions. A more complex model including the possible Dzyaloshinskii–Moriya interaction between A-ions and set of exchange interactions between subsystems was considered in Ref. [13]. Although including these exchange parameters induce modifications, the effective exchange field from B-subsystem on the A-sites at  $T = 2$  K is still the same for both models.

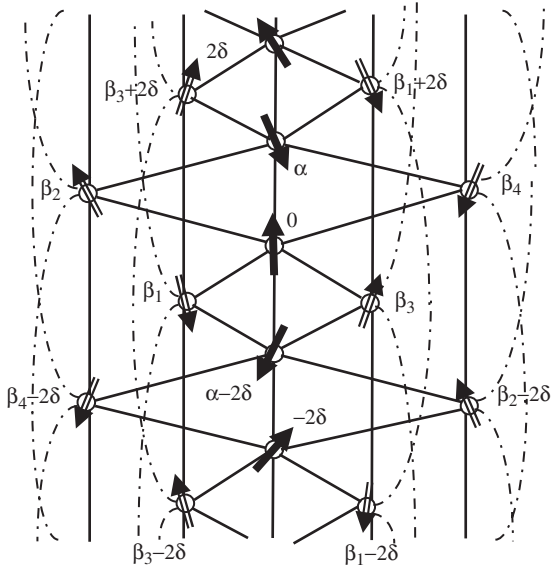


Fig. 1. A simple scheme for the exchange interactions in CuB<sub>2</sub>O<sub>4</sub>. Vertical lines are the AF interaction  $J_a$  within A-subsystem (central line) and the exchange NN interactions within 4 ladders, passed through the each primitive cell of the crystal. Dashed lines—NNN AF interactions within the B-subsystem  $J_{b2}$ .

### 3. Local exchange fields

The transition from the crystal axes  $(x, y, z)$  to the local coordinates of each spin  $(x_i, y_i, z_i)$  is obtained by transforming the pair interactions of Hamiltonian (Eq. (1))

$$\begin{aligned} S_i^x S_j^x + S_i^y S_j^y &= (S_{xi} S_{xj} + S_{yi} S_{yj}) \cos(\alpha_i - \alpha_j) \\ &\quad + (S_{xi} S_{yj} - S_{yi} S_{xj}) \sin(\alpha_i - \alpha_j), \\ S_i^x S_j^y - S_i^y S_j^x &= -(S_{xi} S_{xj} + S_{yi} S_{yj}) \sin(\alpha_i - \alpha_j) \\ &\quad + (S_{xi} S_{yj} - S_{yi} S_{xj}) \cos(\alpha_i - \alpha_j). \end{aligned}$$

The local axis  $x_i$  is directed along the projection of the average spins of  $i$ -ion onto the tetragonal plane,  $z_i = z$  is the tetragonal axis, and  $y_i \perp x_i$ . The simple spiral (SS) structure can be considered as a modulated commensurate AF structure [14]. Hence, the number of independent variables (angles of orientation  $x_i$ -axis within a plane) is equal to the number of ions in the magnetic cell plus the angle-step of the spiral. In CuB<sub>2</sub>O<sub>4</sub> the AF ordering occurs without doubling of the primitive

cell of the crystal. So, the number of angles of AF structure is equal to the number of Cu-ions in the primitive cell. Fixing one angle of A-subsystem as a center point ( $\alpha_0 = 0$ ), we may obtain six independent variables to describe the SS structure in copper metaborate (Fig. 1). The local fields along  $y_i$  direction in the main field approach [15] have the form

$$\begin{aligned} h_y^0 &= 2S_a J_a^{xy} (\sin \alpha + \sin(\alpha - 2\delta)) \\ &\quad + S_{bx} \left( J_{ab} \sum_i \sin \beta_i + D_{ab} (\cos \beta_1 \right. \\ &\quad \left. - \cos \beta_2 + \cos \beta_3 - \cos \beta_4) \right), \\ h_y^{\beta 1} &= -2S_{bx} (\sin(\beta_1 - \beta_3) (J_{b1} \cos 2\delta + D_{b1} \sin 2\delta)) \\ &\quad - S_a (J_{ab} (\sin \beta_1 + \sin(\beta_1 - \alpha + 2\delta)) \\ &\quad - D_{ab} (\cos \beta_1 - \cos(\beta_1 - \alpha + 2\delta))), \\ h_y^{\beta 2} &= -2S_{bx} (\sin(\beta_2 - \beta_4) (J_{b1} \cos 2\delta + D_{b1} \sin 2\delta)) \\ &\quad - S_a (J_{ab} (\sin \beta_2 + \sin(\beta_2 - \alpha)) \\ &\quad + D_{ab} (\cos \beta_2 - \cos(\beta_2 - \alpha))), \\ h_y^{\beta 3} &= h_y^{\beta 1} (\beta_1 \leftrightarrow \beta_3), \quad h_y^{\beta 4} = h_y^{\beta 2} (\beta_2 \leftrightarrow \beta_4), \end{aligned} \quad (2)$$

where  $S_{a,bx}$  are an average spin of A-subsystem and the projection onto the tetragonal plane of the average B-spin accordingly. By elimination of this transverse field, we can evaluate all angles of the initial AF structure through the step of spiral  $\delta$ . Then the longitudinal fields along the  $x_i$ -directions on A- and B-sites have the form

$$\begin{aligned} h_x^A &= -2S_a \left( 2J_a^{xy} \cos \delta + \right. \\ &\quad \left. \frac{(J_{ab} \sin \delta/2 - D_{ab} \cos \delta/2)^2}{J_{b1} \cos 2\delta + D_{b1} \sin 2\delta} \right), \\ h_x^B &= -2S_{bx} (J_{b1} \cos 2\delta \\ &\quad + D_{b1} \sin 2\delta - J_{b2} \cos 4\delta). \end{aligned} \quad (3)$$

This result shows that the addition longitudinal field from B-subsystem on the A-sites  $h_{ax}$  (second term in Eq. (3)) is expressed by the spiral step  $\delta$  and is formally independent on  $S_{bx}$ . The exchange parameters  $J_{ab}, D_{ab}, J_{b1}, D_{b1}, J_{b2}$  were determined by minimization of the part of the free energy that

depends on the spiral step

$$\delta F_1 = 2S_a \delta h_x^A + 4S_{bx} \delta h_x^B$$

for the known temperature dependence of the incommensurability vector  $q_0(T)$  [4]. The value of the exchange interaction between A-spins  $J_a^{xy} = 45$  K is derived from the analysis of the SW spectrum at  $T = 12$  K [10]. In A-subsystem the site magnetization can be assumed to be equal to the constant value  $g\mu_B S_a = 0.9 \mu_B$  in the temperature range  $2 \text{ K} < T < 12 \text{ K}$ . In B-subsystem, the magnetic moment size changes from  $0.2 \mu_B$  at  $T = 12$  K to  $m_b^0 = 0.54 \mu_B$  at  $T = 2$  K and can be approximated by the Brillouin function

$$m_b = m_b^0 \text{th} \frac{m_b T_{N2}}{m_b^0 T}, \quad (4)$$

where  $T_{N2} = 12.6$  K—is the temperature of the macroscopic magnetization arising in the B-subsystem. The reorientation of the B-moments from tetragonal axis  $z$  at  $T = 12$  K to the intermediate direction with the angle from  $z$   $\Theta_0 \approx \pi/2.7$  at  $T = 2$  K [3] was approximated by different power functions of temperature

$$\Theta = \Theta_0(1 - T/T^*)^\gamma, \quad (5)$$

where  $T^*$  is the temperature at which the reorientation starts. The quantitative agreement between theoretical and experimental dependences of  $q_0(T)$  was obtained for some sets of the exchange parameters for a different power  $\gamma$ . For all sets of parameters, the relative mean field of the intersubsystem interactions (the second term in Eq. (3))  $h_{ab}^{mf}$  at  $T = 2$  K was still almost constant.

$$h_{ab}^{mf}(T) = \frac{h_{ab}(\delta)}{nSJ_a^{xy}} = \frac{2(J_{ab} \sin \delta/2 - D_{ab} \cos \delta/2)^2}{nJ_a^{xy}(J_{b1} \cos 2\delta + D_{b1} \sin 2\delta)} = 0.022 \pm 0.003 \quad (T = 2 \text{ K}), \quad (6)$$

where  $n = 4$ —a number of the NN in the A-subsystem.

#### 4. Spin-wave theory

The analysis of the upper (high energy) branches in the spin-wave spectrum of copper metaborate

can be done in the framework of the linear approach as it was done for  $T > 10$  K [10]. The Hamiltonian of the “easy plane” antiferromagnetic subsystem A in the local axes  $(x_i, y_i, z_i)$  has the form

$$H = J_a^z \sum_{ij} S_{zi} S_{zj} + J_a^{xy} \times \sum_{ij} \left( \cos(\alpha_i - \alpha_j)(S_{xi} S_{xj} + S_{yi} S_{yj}) + \sin(\alpha_i - \alpha_j)(S_{xi} S_{yj} - S_{yi} S_{xj}) \right) + h_{ax}(q_0) \sum_i S_{xi}. \quad (7)$$

The part in the Hamiltonian that is quadratic in the quantization operators after the Holstein–Primakoff transformation [16] in the local axes

$$S_{xi} = S - b_i^+ b_i,$$

$$S_{yi} = \sqrt{\frac{S}{2}}(b_i^+ + b_i),$$

$$S_{zi} = i\sqrt{\frac{S}{2}}(b_i - b_i^+) \quad (8)$$

becomes

$$H_2 = A \sum_i b_i^+ b_i - B \sum_{ij} b_i^+ b_j - C \sum_{ij} (b_i^+ b_j^+ + h.c.),$$

$$A = nSJ_a^{xy} \cos \delta + h_{ax}(\delta),$$

$$B = \frac{S}{2}(J_a^{xy} \cos \delta - J_z),$$

$$C = \frac{S}{2}(J_a^{xy} \cos \delta + J_z).$$

The Fourier transform

$$b_{ij} = \frac{1}{\sqrt{N}} \sum_k b_{1k,2k} \exp(i\vec{k}\vec{r}_{ij}),$$

where  $\vec{k}$  is a vector in reciprocal space, leads to the momentum representation of the Hamiltonian

$$\begin{aligned}
 H_2 = & \sum_k (A(b_{1k}^+ b_{1k} + b_{2k}^+ b_{2k}) - 2B(B_k b_{1k}^+ b_{2k} + h.c.) \\
 & - 2C(B_k b_{1k}^+ b_{2-k}^+ + h.c.)), \\
 B_k = & \exp(-i\vec{k} \cdot \vec{c}/4) \cos(\vec{k} \cdot \vec{b}/2) \\
 & + \exp(i\vec{k} \cdot \vec{c}/4) \cos(\vec{k} \cdot \vec{a}/2), \quad (9)
 \end{aligned}$$

where indexes 1 and 2 are related to different AF sublattices. After separation on independent optical and acoustical branches and diagonalization of the square-law part, we obtain two SW branches with eigenenergies

$$\begin{aligned}
 E_k^{a,c} \\
 = & \sqrt{(A \mp 2(B+C)\sqrt{B_k B_k^*})(A \mp 2(B-C)\sqrt{B_k B_k^*})}. \quad (10)
 \end{aligned}$$

### 5. Comparison with the experiment and discussion

Because there are two types of SS domains due to tetragonal symmetry of the chemical structure with wave-vector propagating in  $z$  and  $-z$  directions, we are actually measuring contributions from both the  $q_0$  and  $-q_0$  domains. We measured the spin-wave spectrum along the high-symmetry directions  $[q, q, 0]$ ,  $[q, q, q]$  and  $[0, 0, q]$ . So, in the crystal reciprocal space  $\vec{q}$

$$\vec{k} = \vec{q} \pm \vec{q}_0,$$

where  $q_\perp$  and  $q_z$  are  $\frac{2\pi}{a}h$ ,  $\frac{2\pi}{c}l$  and  $h$  and  $l$  are the Miller indices, Eq. (10) simplifies to

$$\begin{aligned}
 \frac{E_k^{a,c}}{nSJ_a^{xy}} \\
 = & \sqrt{(\cos \delta (1 \mp \cos((q_z \pm q_0)c/4) \cos(q_\perp a/2)) + h_s(\delta))} \\
 & \times \sqrt{(\cos \delta \pm (J_a^-/J_a^{xy}) \cos((q_z \pm q_0)c/4) \cos(q_\perp a/2) + h_s(\delta))}. \quad (11)
 \end{aligned}$$

where  $h_s(\delta) = h_{ax}(\delta)/nSJ_a^{xy}$ . Fig. 2 summarizes our results at  $T = 2$  K. As for  $T = 12$  K from our experimental data, we have only clear evidence for the acoustic dispersion branch because the intensity of the optical branch is weak [10].

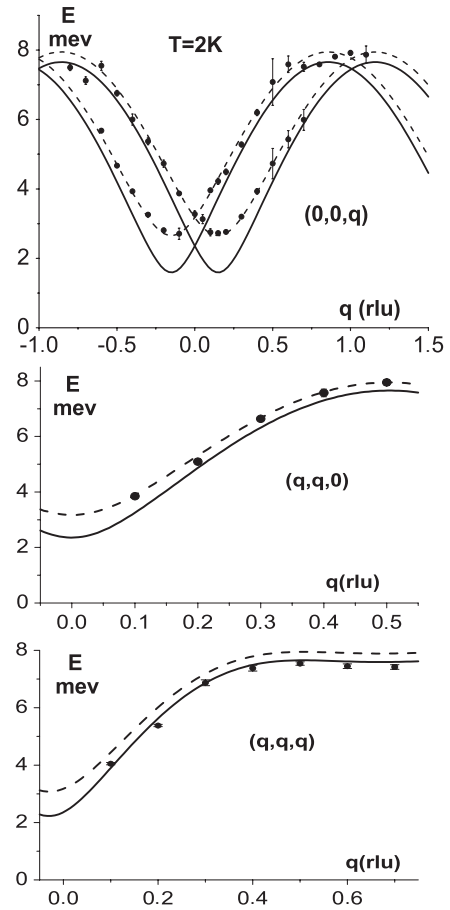


Fig. 2. Spin-wave spectrum of  $\text{CuB}_2\text{O}_4$  at  $T = 2$  K. Circles—experimental data points obtained from inelastic neutron scattering, solid and dash lines—result of the theoretical analysis in the framework of the mean field theory and with the additional Ising-like “spiral anisotropy” (see the text), respectively for  $(0, 0, q)$ ,  $(q, q, 0)$  and  $(q, q, q)$  directions.

In agreement with the crystalline structure of copper metaborate, the SW energy at the zone boundary  $q_z c = 1$ ,  $q_\perp a = 0$  is equal to the energies at the boundaries  $q_z c = 0$ ,  $q_\perp a = 0.5$  and  $q_z c = q_\perp a = 1$  in the energy resolution limits. The experimental value of the energy gap  $\Delta E(\vec{q}_0) \sim 2.7$  meV is larger than the theoretical one that is obtained from the mean field result (11) (solid line in Fig. 2). This discrepancy is due to the mean-field approach that neglects the dynamical interaction between subsystems through the

fluctuations of the magnetic moments (“order due to disorder” mechanism [17]). The dynamical interaction between two subsystems with frustration of the intersubsystem exchange interactions leads to the appearance of a temperature dependent anisotropy in the exchange interaction within subsystems (Shender collinearity) [18]. As it was shown in Ref. [19], this anisotropy “should create a gap in the pseudo-Goldstone mode . . . , which has gapless at  $\vec{k} = 0$  in harmonic order”. Such Ising-like anisotropy favors a collinear orientation of the magnetic moments in the different subsystems [20] and in our case this mechanism must lead to the additional effective Ising-like interaction between the A-spins which follows from the orientations of the B-spins. In the spiral phase this anisotropy field turns within the tetragonal plane when shifting along the  $z$ -axis, i.e. an additional “spiral anisotropy” (SA) appears. Taking into account this anisotropy by adding the Ising-term in the Hamiltonian (7)

$$H_I = aJ_a^{xy} \sum_{ij} S_{xi} S_{xj}, \quad (12)$$

we obtain the total SA field

$$h_{ax} = h_{ab}(q_0) + a(T)nSJ_a^{xy}, \quad (13)$$

where  $h_{ab}(q_0)$  is a static mean field (6). The good agreement between experimental data and SW energy (11,13) (Fig. 2, dashed lines) was obtained for the relative total field  $h_s(T = 2 \text{ K}) = 0.06$ . So, the dynamical Ising-like part of the effective SA can be estimated as  $a(T = 2 \text{ K}) = 0.038$ . In order to estimate the temperature dependence of  $a(T)$ , we compare the SW spectrum (11,13) with the experimental data at  $T = 12 \text{ K}$ . At this temperature the wave vector of the incommensurate structure (and the spiral step  $\delta$ ) has become extremely small  $q_0 \leq 0.02 \text{ rlu}$ . As a result the frustration-breaking mean field decreases too:  $h_{ab}^{mf}(T = 12 \text{ K}) = 0.0008$ . So, at  $T = 12 \text{ K}$  the theoretical curves are in agreement with experimental data for  $a(T = 12 \text{ K}) = 0$  (Fig. 3). Note, that accounting for the field  $h_{ab}^{mf}(q_0 = 0.02 \text{ rlu})$  improves the agreement between the theoretical and experimental results in comparison with SW theory for the pure “easy-plane” AF [8].

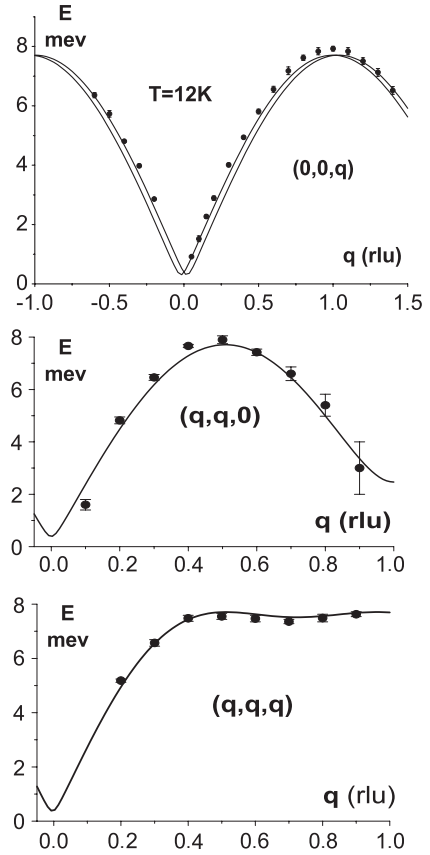


Fig. 3. Spin-wave spectrum of  $\text{CuB}_2\text{O}_4$  at  $T = 12 \text{ K}$ . Two branches for  $(0,0,q)$  direction correspond to the two spiral domains (see the text).

## 6. Conclusion

We have investigated the spectrum of magnetic excitations in copper metaborate in the incommensurate magnetic phase at  $T = 2 \text{ K}$ . The influence of the intersubsystem interactions on the spin dynamics of the 3d-ordered magnetic subsystem A was considered in the framework of mean field theory as the frustration-breaking longitudinal field. This field creates a gap in the SW spectrum at the incommensurate vector  $\pm q_0$ . The comparison with results of inelastic neutron scattering experiments showed that in the incommensurate phase  $T < 10 \text{ K}$  an additional mechanism of “spiral anisotropy” appears, which increases the SW

energy gap. We assumed that this mechanism has a dynamical (fluctuational) origin (so called “order due to disorder”) analogous to the Ising-like additional interaction in another two-subsystem magnetism with the frustration of the interactions between subsystems.

### Acknowledgements

This work is done under partial support from RFBR (Grant 03-02-16701). We also thank M. Popov and A. Pankrats for fruitful discussions and L.P. Regnault for his help in setting up the experiment on IN22.

### References

- [1] G.A. Petrakovskii, D. Velikanov, A. Vorotinov, K. Sablina, A. Amato, B. Roessli, J. Schefer, U. Staub, *J. Magn. Magn. Mater.* 205 (1999) 105.
- [2] B. Roessli, J. Schefer, G.A. Petrakovskii, B. Ouladdiaf, M. Boehm, U. Staub, A. Vorotinov, L. Bezmaternikh, *Phys. Rev. Lett.* 85 (2001) 1885.
- [3] M. Boehm, B. Roessli, J. Schefer, A. Furrer, A. Wills, B. Ouladdiaf, B. Lelievre-Berna, U. Staub, G.A. Petrakovskii, *Phys. Rev. B* 68 (2003) 024405.
- [4] G.A. Petrakovskii, A.I. Pankrats, M.A. Popov, et al., *Low Temp. Phys.* 28 (2002) 606.
- [5] A.I. Pankrats, G.A. Petrakovskii, M.A. Popov, et al., *JETP Lett.* 78 (2003) 569.
- [6] R.V. Pisarev, I. Sanger, G. Petrakovskii, M. Fiebig, *Phys. Rev. Lett.* 93 (2004) 037204.
- [7] H. Nakamura, Y. Fujii, H. Kikuchi, et al., *EASTMAG-2004, Abstract, Krasnoyarsk, 2004*, p. 51.
- [8] K.M. Kojima, Y. Fudamoto, M. Larkin, et al., *Phys. Rev. Lett.* 78 (1997) 1787.
- [9] E.M. Lifshitz, L.P. Pitaevskii, *Statistical Physics, Part 2*, Fizmatlit, Moscow, 2001.
- [10] M. Boehm, S. Martynov, B. Roessli, G. Petrakovskii, J. Kulda, *J. Magn. Magn. Mater.* 250 (2002) 313.
- [11] S. Martynov, G. Petrakovskii, B. Roessli, *J. Magn. Magn. Mater.* 269 (2004) 106.
- [12] M.A. Popov, G.A. Petrakovskii, V.I. Zinenko, *Fiz. Tverd. Tela* 46 (2004) 478.
- [13] S.N. Martynov, *Physics of the Solid State*, 47 (2005) 678. (Translated from *Fizika Tverdogo Tela*, 47 (2005) 654).
- [14] Yu.A. Izyumov, *Diffraction of Neutrons on Diffraction of Neutrons Long-period Structures*, Energoatomizdat, Moscow, 1987 [In Russian].
- [15] J.S. Smart, *Effective Field Theories of Magnetism*, W.B. Saunders Company, Philadelphia, London, 1966.
- [16] S.V. Tyablikov, *Methods of Quantum Theory of Magnetism*, Nauka, Moscow, 1975 [In Russian].
- [17] J. Villain, R. Bidaux, J.P. Carton, R. Conte, *J. Phys. (Paris)* 41 (1980) 1263.
- [18] E.F. Shender, *Sov. Phys. JETP* 56 (1982) 178.
- [19] C.L. Henley, *Phys. Rev. Lett.* 62 (1989) 2056; C.L. Henley, *Phys. Rev. Lett.* 73 (1994) 2788.
- [20] Y.J. Kim, A. Aharony, R.J. Birgeneau, et al., *Phys. Rev. Lett.* 83 (1999) 852.